The Canadian Mineralogist
Vol. 33, pp. 165-184 (1995)

DISTRIBUTION OF PLATINUM-GROUP ELEMENTS IN THE NIQUELÂNDIA LAYERED MAFIC–ULTRAMAFIC INTRUSION, BRAZIL: IMPLICATIONS WITH RESPECT TO EXPLORATION

CESAR F. FERREIRA FILHO*, ANTHONY J. NALDRETT AND MOHAMMAD ASIF

Department of Geology, University of Toronto, 22 Russell Street, Toronto, Ontario M5S 3B1

ABSTRACT

The study of the distribution of PGE, Au, Ni, Cu, Co, and S in the Proterozoic Niquelândia mafic–ultramafic layered intrusion (Brazil), 65 km long and 35 km wide, shows the existence of two distinct stratigraphic zones of contrasting PGE content. The Ultramafic Unit and the lowermost part of the Central Mafic Unit have relatively high PGE contents, whereas all units above this level have very low PGE contents. Data on sulfur contents, as well as the presence of interstitial base-metal sulfides starting from the intermediate level of the Ultramafic Unit, suggest that the parental magma was close to the saturation level, and that sulfur saturation occurred during fractional crystallization of the magma. The observed distribution of the precious metals is modeled in terms of the depletion of the magma in its PGE content due to the segregation of a sulfide liquid. The transition zone between PGE-undepleted and PGE-depleted rocks is considered to be the most favored stratigraphic level for stratiform PGE deposits in the Niquelândia Layered Intrusion. Similar to many PGE-mineralized units in layered intrusions, the transition zone occurs close to the level at which plagioclase first appears as a dominant cumulus phase; this emphasizes the potential for magmatic PGE deposits at this stratigraphic level in the Niquelândia Layered Intrusion.

Keywords: geochemistry, layered intrusion, PGE, platinum-group elements, precious metals, sulfide saturation, chromitite, Niquelândia Layered Intrusion, Brazil.

SOMMAIRE

Notre étude de la distribution des éléments du groupe du platine (EGP), Au, Ni, Cu, Co et S dans le massif intrusif protérozoïque de Niquelândia (Brésil), 65 km de long et 35 km de large, démontre l'existence de deux zones stratigraphiques à teneurs distinctes en EGP dans la séquence mafique – ultramafique. L'unité ultramafique, à la base, et la partie inférieure de l'unité mafique centrale ont une teneur en EGP relativement élevée, tandis que toutes les unités supérieures en sont appauvries. Les données sur la concentration du soufre, ainsi que la présence de sulfures interstitiels de métaux de base à partir d'un niveau intermédiaire de l'unité ultramafique, font penser que le magma parental était tout près de la saturation en soufre, qui en fait a été atteinte au cours de sa cristallisation fractionnée. La distribution observée des métaux précieux pourrait bien résulter d'un appauvrissement du magma en EGP à cause de la séparation d'un liquide sulfuré. La zone de transition entre roches non appauvries et roches appauvries serait le niveau le plus favorable pour découvrir les dépôts stratiformes qui pourraient se trouver dans ce massif intrusif. Tout comme dans les unités minéralisées en EGP de plusieurs complexes stratiformes, la transition est proche du niveau où le plagioclase devient la phase cumulative dominante. Cette coïncidence souligne le potentiel pour des gisements magmatiques d'EGP près de ce niveau dans le complexe stratiforme de Niquelândia.

(Traduit par la Rédaction)

Mots-clés: géochimie, massif intrusif stratiforme, éléments du groupe du platine, métaux précieux, saturation en sulfures, chromitite, complexe stratiforme de Niquelândia, Brésil.

INTRODUCTION

In recent years, many studies have focused on the geochemistry of platinum-group elements (PGE) in mineralized units within layered mafic–ultramafic intrusions. Some of these studies have focused on the behavior of PGE during the crystallization of layered intrusions, in order to understand the controls on distribution of the PGE (Hoatson & Keays 1989, Naldrett & von Gruenewaldt 1989, Naldrett *et al.* 1990). A particular aim in these studies is to use the distribution of the PGE as an exploration tool that can define the most favorable stratigraphic level for sulfide saturation and PGE concentration.

On the other hand, few data are available on the distribution of precious metals in unmineralized

* Present address: Instituto de Geociências, Universidade de Brasília, Brasília, DF, 70.910, Brazil.

layered intrusions. In this paper, we present new geochemical data for the Niquelândia layered mafic–ultramafic intrusion (NLI), in Brazil. The results are used to study the behavior of PGE + Au in this exhumed magma-chamber and to evaluate the potential for PGE mineralization. Previous studies on whole-rock geochemistry of precious metals in the NLI include those of White *et al.* (1971) and Sighinolfi *et al.* (1983). Our study presents results on trace-element geochemistry for a larger number of samples, covering all the NLI units, and contains the first data-set for Os and Ir. The current limits of detection for the PGE are much lower than in the previous studies.

Regional Geological Setting

Figure 1 shows the main tectonic units of the north–central Goiás region, in the central part of Brazil. The mafic and ultramafic intrusions form a linear array within Proterozoic folded belts exposed between two major cratonic regions (Amazon and São Francisco cratons). The main units present in the area are:

1) Neoproterozoic sedimentary belts: They include the Brasília Belt at the western margin of the São Francisco craton. The Brasília Belt was deformed during the Brasiliano orogenic cycle (*ca.* 650 Ma) and exhibits a tectonic polarity, with tectonic and metamorphic vergence toward the stable cratonic area (Marini *et al.* 1984).

2) Uruaçu Belt: This is a polydeformed psammitic–pelitic sequence with interlayered volcanic rocks metamorphosed to the greenshist to amphibolite facies (Marini *et al.* 1984). Recent dating (Pimentel *et al.* 1992) indicates a Neoproterozoic age for the belt, which represents an internal facies of the Brasília Belt.

3) Goiás Massif: This consists of older basement rocks that are variably affected by the Brasiliano cycle deformation and metamorphism (Marini *et al.* 1984). The massif includes typical Archean granite–greenstone belt terranes and is interpreted to be a mosaic of tectonic blocks with different ages and tectonic evolutions (Fuck *et al.* 1987, Brito Neves & Cordani 1991).

4) Araí Group: This is a continental sedimentary sequence with a thick rhyolitic unit at the base (Marini *et al.* 1984). U–Pb (zircon) ages of 1770 Ma are reported for both rhyolitic volcanism and associated tin-bearing granites (Pimentel *et al.* 1991), indicating a magmatic–sedimentary activity in an extensional

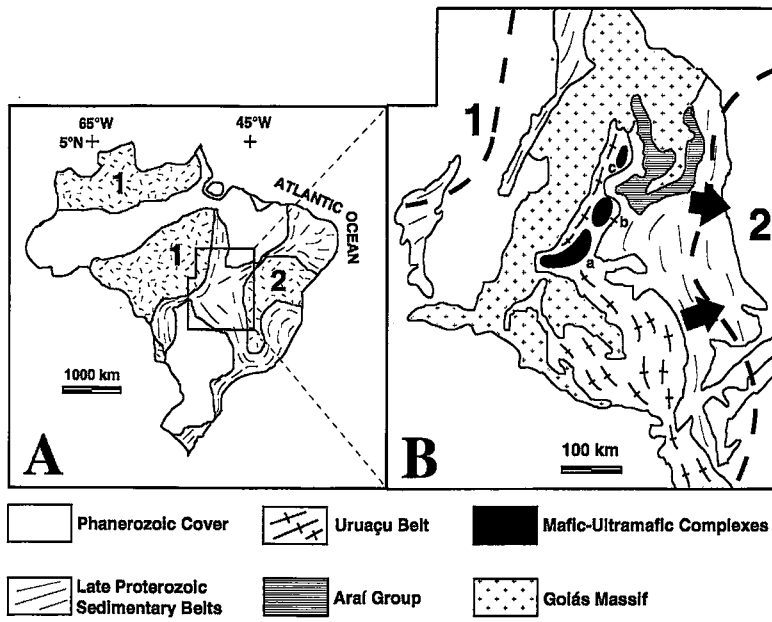

FIG. 1. A) Main geotectonic units in Brazil. The outlined area is shown in detail in B. Dashed lines indicate regions affected by the Upper Proterozoic (Brasiliano) geodynamic cycle. B) Geological sketch-map of central Brazil. Dashed lines indicate limit of cratonic areas. 1: Amazonian Craton, 2: São Francisco Craton. Arrows indicate tectonic vergence of supracrustal rocks. a: Barro Alto Complex, b: Niquelândia Complex, c: Cana Brava Complex. Based on Danni *et al.* (1982), Marini *et al.* (1984), and Pimentel *et al.* (1991).

intracratonic tectonic setting.

5) Layered intrusions: The three major layered intrusions (Barro Alto, Niquelândia and Cana Brava) are deformed, high-grade metamorphic complexes (Danni *et al.* 1982). U–Pb isotopic data for the NLI (Ferreira Filho *et al.* 1993, Ferreira Filho *et al.* 1994) suggest a Mesoproterozoic age (1560–1600 Ma) for magmatic emplacement and set a Neoproterozoic age for the metamorphism (770–795 Ma). A major Mesoproterozoic continental rift is suggested for the 350-km-long belt of layered intrusions in the region, whereas the high-grade metamorphism and associated deformation are correlated with a Neoproterozoic continental collision (Ferreira Filho & Naldrett 1993).

Geology of the Niquelandia Layered Intrusion

The geology of the Niquelândia Layered Intrusion (NLI) was reviewed by Ferreira-Filho *et al.* (1992c). The NLI, located in central Brazil, is about 1,800 square km in area and an estimated 10–15 km in thickness; it is among the largest layered mafic–ultramafic intrusions in the world. The NLI is delineated by fault zones to the north, south and east (Fig. 2), where it is in contact with mylonitic gneisses

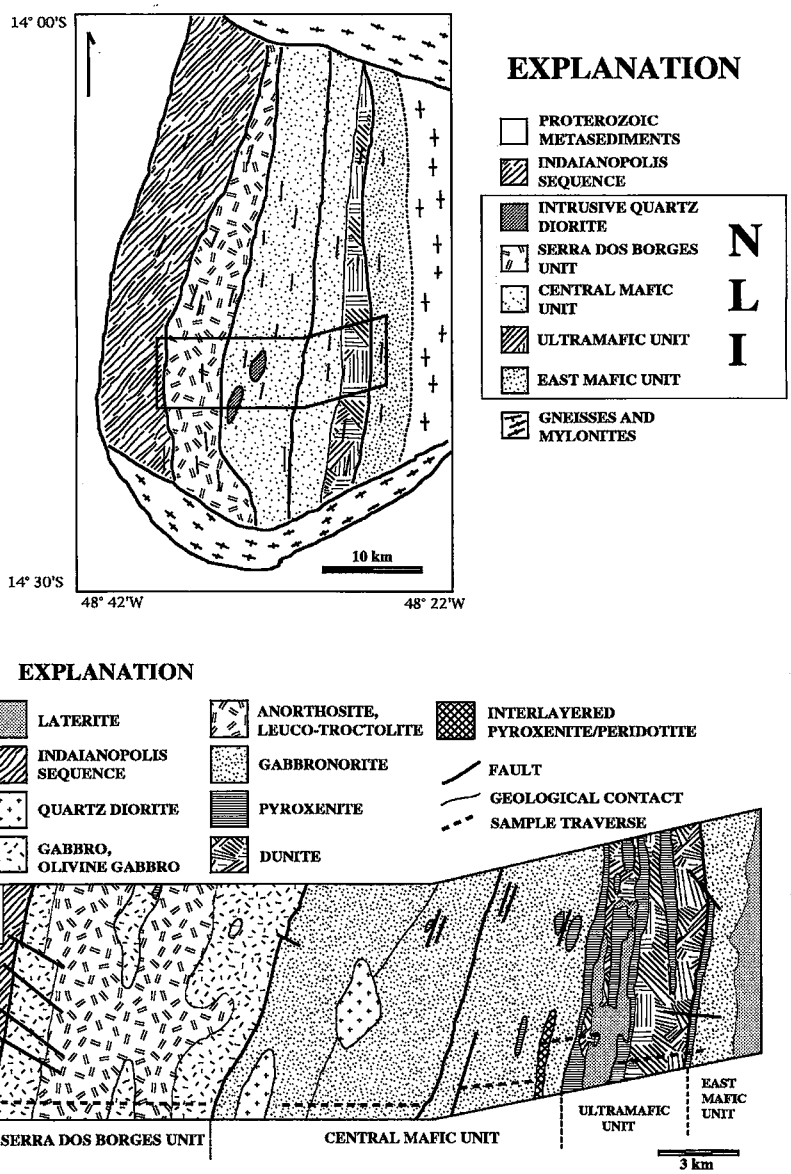

FIG. 2. Geology of the Niquelândia Layered Intrusion (NLI). From Ferreira Filho *et al.* (1992c).

interpreted to be faulted country-rocks. The stratigraphy of the NLI comprises four westward-dipping major units, with a gradation from a more primitive base, where olivine and pyroxene cumulates predominate, toward a more differentiated top, where plagioclase cumulates predominate.

The East Mafic Unit (EMU), on the intrusion's eastern border, consists mainly of gabbronorite with interlayered websterite, plagioclase websterite and norite. These rock types are usually transformed to a fine-grained granoblastic aggregate (a granulitic blastomylonite); primary minerals and textures only rarely are preserved. The unit is interpreted to be a border group (Girardi *et al.* 1986), which is supported by the stratigraphic position and by the relatively more primitive nature of the gabbroic rocks.

The Ultramafic Unit (UMU) consists mainly of dunite ± harzburgite (olivine + chromian spinel cumulate) and pyroxenite [orthopyroxene (opx) or opx + clinopyroxene (cpx) cumulate]. The sequence of crystallization of the early-formed cumulus phases in the NLI is olivine, orthopyroxene, clinopyroxene and plagioclase. Although orthopyroxene preceded clinopyroxene, as indicated by orthopyroxenite with intercumulus clinopyroxene, clinopyroxene appears early in the NLI. This is indicated by the predominance of websterite (opx + cpx cumulate) over orthopyroxenite (opx cumulate with intercumulus cpx) in the UMU. Dunite predominates at the base, with interlayered pyroxenite beds gradually increasing toward the top. Lherzolite, gabbronorite, norite and thin layers of chromitite are subordinate. The chromitite seams of the UMU were described by White *et al.* (1971) and Figueiredo (1977). Platinum-group minerals (PGM) have been described in the NLI chromitites by Ferrario & Garuti (1988) and Millioti & Stumpfl (1993). The chromite-hosted PGM occur as primary inclusions of sulfides (laurite, erlichmanite) and alloys (iridosmine, platinum–iron alloy). The primary composition of olivine varies irregularly in the UMU from Fo_{92} to Fo_{85} (Girardi *et al.* 1986). Both the cryptic variation of olivine and the presence of cyclic units suggest that the UMU is formed by successive influxes of new magma. The UMU has an estimated thickness of 1–2 km.

The Central Mafic Unit (CMU) has an estimated thickness of 5–7 km and consists of gabbronorite (± norite) with interlayered ultramafic beds. The contact with the UMU to the east is gradational, and marks the appearance of cumulus plagioclase as one of the dominant mineral phases. Cumulus Mg-rich olivine (Fo_{84-92}), which is still present in some of the ultramafic interlayered beds, together with chromian spinel, disappears 1,000 meters above the base of the CMU.

The Serra dos Borges Unit (SBU) has an estimated thickness of 4–6 km and consists of interlayered "gabbroic" rocks (gabbro, gabbronorite, olivine gabbro) and "anorthositic" rocks (anorthosite, leucotroctolite, leucogabbro, leucogabbronorite). Although invariably interlayered, the "gabbroic" rocks predominate at the base of the unit, whereas the "anorthositic" rocks predominate at the top. The SBU marks the re-appearance of olivine (Fo_{63-76}); it has thin layers of magnetite–ilmenite ore.

The inferred composition of the parental magma, based on bulk-rock chemistry of the cumulates, is that of a low-Ti picritic basalt (Girardi *et al.* 1986). The inferred $Mg/(Mg + Fe^{2+})$ ratio of liquids in equilibrium with the most Mg-rich olivine span the range from 0.77 to 0.70 (Girardi *et al.* 1986).

The most important tectonic feature in the NLI is the presence of NS–N10E zones of ductile shear (Ferreira Filho *et al.* 1992c). Within these zones (up to hundreds of meters wide), tectonic foliation and high-grade metamorphic paragenesis are developed. The heterogeneous nature of the deformation and metamorphic recrystallization is indicated by the presence of shear zones within areas of primary igneous texture and mineralogy. Based on the association of metamorphic minerals developed within the shear zones, the NLI can be divided into three metamorphic zones: enstatite granulite, hornblende granulite and amphibolite, with metamorphism increasing progressively from west to east (Ferreira Filho *et al.* 1992b). The progressive nature of the metamorphism is also indicated by the gradational change in composition of the metamorphic amphibole. Thermobarometric calculations indicate a temperature of 800–900°C and a pressure of 7–8 kbar for the higher-grade rocks, where the assemblage hercynite + quartz is stable (Ferreira Filho *et al.* 1992a).

Sample Selection

The analyses for PGE, Au, Cu, Ni, Co and S were made on a suite of 54 samples representing an east–west section across the intrusion. All samples were taken from outcrops within the area mapped in detail by Ferreira Filho *et al.* (1992c) and have primary igneous mineralogy and texture. Most of the olivine-rich peridotite was partially overprinted by later serpentinization, and the use of partially serpentinized rocks was unavoidable. The four samples of chromitite are partially weathered; they were collected from old exploration trenches.

A petrographic description of the analyzed samples can be found in Appendix 1, whereas the typical textures of the rock types being considered in our study are illustrated in Figure 3.

Analytical Techniques

Whole-rock samples were analyzed for Ni, Co, Cu, and S by atomic absorption spectroscopy at INCO Geological Research Laboratories (Copper Cliff,

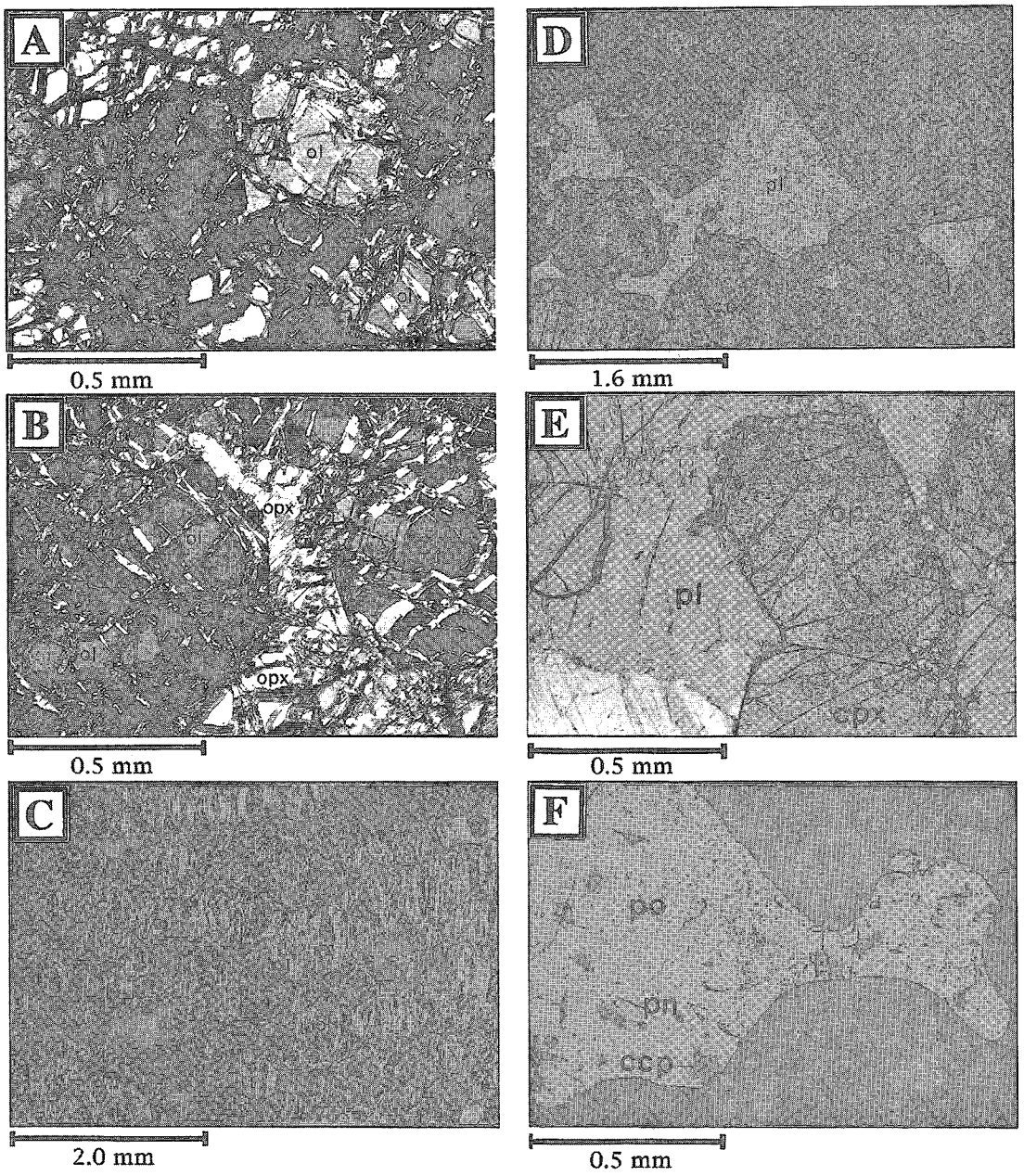

FIG. 3. A) Partially serpentinized dunite (ol ± chr cumulate) of the UMU. Adcumulate texture. Crossed nicols. B) Partially serpentinized harzburgite (ol cumulate with intercumulus opx) of the UMU. Mesocumulate texture. Crossed nicols. C) Mostly serpentinized dunite (ol ± chr cumulate) of the UMU. Even though olivine is mostly replaced by serpentine, the adcumulate texture is preserved. Plane-polarized light. D) Websterite (opx + cpx cumulate with intercumulus pl) of the UMU. Mesocumulate texture. Plane-polarized light. E) Gabbronorite (opx + cpx + pl cumulate) of the CMU. Plane-polarized light. F) Websterite (opx + cpx cumulate) with interstitial sulfide of the CMU. Dominant sulfide is pyrrhotite with minor pentlandite and chalcopyrite. Plane-polarized light.

Ontario). Concentrations of the PGE and Au were determined by Ni-sulfide fire-assay preconcentration followed by instrumental neutron-activation analysis (INAA) at the University of Toronto. The samples were irradiated at the Nuclear Reactor Center of McMaster University (Hamilton, Ontario). The detec-

TABLE 1. CONCENTRATION OF PGE, Au, Ni, Cu, Co AND S: EAST–WEST SECTION ACROSS THE NIQUELÂNDIA LAYERED INTRUSION

Sample	Unit	Rock	Cu	Ni	Co	S	Pt	Pd	Rh	Ru	Ir	Os	Au	Pt/Ir
CF54	SBU	Gb	135	205	0.006	0.09	1.8	<2	<0.1	<0.5	0.05	<0.3	0.6	36.0
CF53	SBU	Gb	90	240	0.008	0.06	1.0	<2	<0.1	<0.5	0.07	<0.3	<0.4	14.3
CF52	SBU	Gb	45	195	0.006	0.03	<1	<2	<0.1	<0.5	0.07	<0.3	<0.4	<14.3
CF51	SBU	Gb	90	160	0.006	0.12	<1	<2	<0.1	<0.5	0.05	<0.3	<0.4	<20.0
CF50	SBU	Gb	30	90	0.005	<0.02	<1	<2	<0.1	3.4	0.07	<0.3	<0.4	<14.3
CF49	SBU	Gb	70	275	0.008	0.04	1.3	<2	<0.1	<0.5	0.14	<0.3	<0.4	9.3
CF48	SBU	Py	40	130	0.005	0.03	<1	<2	<0.1	3.0	0.02	<0.3	<0.4	<50.0
CF47	SBU	Py	55	160	0.006	0.04	<1	<2	<0.1	<0.5	0.04	<0.3	<0.4	<25.0
CF46	SBU	Gb	150	225	0.005	0.06	<1	<2	<0.1	<0.5	0.03	<0.3	<0.4	<33.3
CF45	SBU	Gb	20	40	0.001	<0.02	<1	<2	<0.1	<0.5	0.01	<0.3	<0.4	<100.0
CF44	SBU	Gb	15	30	<0.001	<0.02	<1	<2	<0.1	<0.5	0.02	<0.3	<0.4	<50.0
CF43	SBU	Gb	110	235	0.005	0.12	<1	<2	<0.1	<0.5	0.02	<0.3	<0.4	<50.0
CF42	SBU	Gb	70	180	0.004	0.06	<1	NA	NA	<0.5	0.03	<0.3	<0.4	<33.3
CF41	SBU	Gb	10	80	0.004	<0.02	<1	<2	<0.1	<0.5	0.04	<0.3	<0.4	<25.0
CF40	CMU	Gb	45	85	0.004	0.11	<1	<2	<0.1	<0.5	0.03	<0.3	0.8	<33.3
CF39	CMU	Gb	45	50	0.005	0.09	NA	NA	NA	NA	NA	NA	NA	NA
CF38	CMU	Gb	25	125	0.005	<0.02	1.4	<2	<0.1	<0.5	0.05	<0.3	2.1	28.0
CF37	CMU	Py	80	115	0.007	0.15	1.9	<2	<0.1	0.8	0.06	<0.3	<0.4	31.7
CF36	CMU	Py	140	480	0.006	0.14	2.2	<2	<0.1	<0.5	0.06	<0.3	1.4	36.7
CF35	CMU	Gb	25	40	0.005	0.19	<1	<2	<0.1	<0.5	0.03	<0.3	0.9	<33.0
CF34	CMU	Gb	50	65	0.004	0.12	NA	<2	<0.1	NA	NA	NA	NA	NA
CF33	CMU	Py	135	565	0.007	0.18	2.7	NA	NA	0.8	0.13	<0.3	2.9	20.8
CF32	CMU	Gb	55	170	0.005	0.11	6.7	<2	0.48	<0.5	0.05	<0.3	0.6	134.0
CF31	CMU	Py	170	465	0.005	0.24	2.6	3.2	<0.1	<0.5	0.05	<0.3	1.6	52.0
CF30	CMU	Gb	50	95	0.005	0.16	<1	<2	<0.1	<0.5	0.04	<0.3	0.5	<25.0
CF29	CMU	Gb	60	95	0.005	0.07	<1	<2	<0.1	<0.5	0.06	<0.3	0.5	<16.7
CF28	CMU	Pe	65	1540	0.013	0.06	30.8	41.4	1.90	3.0	0.64	0.4	29.8	48.1
CF27	CMU	Pe	60	850	0.009	0.04	NA	NA	NA	NA	NA	NA	NA	NA
CF26	CMU	Gb	30	50	0.005	0.15	1.5	NA	NA	<0.5	0.03	<0.3	0.4	50.0
CF25	CMU	Py	145	410	0.006	0.11	4.3	<2	<0.1	2.9	0.12	<0.3	1.4	35.8
CF24	CMU	Py	435	1030	0.007	0.27	<1	<2	NA	NA	NA	NA	NA	NA
CF23	UMU	Py	145	405	0.005	0.17	2.6	NA	NA	1.2	0.04	<0.3	0.7	65.0
CF22	UMU	Py	175	475	0.009	0.44	<1	NA	NA	1.5	0.04	<0.3	1.1	<25
CF21	UMU	Pe	55	1030	0.013	0.03	23.9	79.8	9.44	4.1	1.13	0.4	21.4	21.1
CF20	UMU	Py	75	530	0.006	0.03	10.9	13.3	1.17	3.5	0.34	0.4	2.2	32.1
CF19	UMU	Cr	30	665	0.009	<0.02	13.5	12.3	12.04	70.7	49.50	39.4	<0.4	0.3
CF18	UMU	Cr	35	885	0.016	<0.02	NA	NA	NA	NA	NA	NA	NA	NA
CF17	UMU	Cr	30	440	0.007	<0.02	9.7	11.0	6.24	18.2	13.05	10.0	<0.4	0.7
CF16	UMU	Cr	35	625	0.012	<0.02	11.6	10.3	8.06	27.3	18.84	9.3	<0.4	0.6
CF15	UMU	Pe	80	970	0.009	0.05	3.0	<2	0.14	<0.5	0.03	<0.3	0.8	100.0
CF14	UMU	Pe	140	715	0.007	0.18	3.2	9.0	0.38	1.0	0.16	<0.3	1.5	20.0
CF13	UMU	Py	230	540	0.005	0.19	3.4	<2	0.23	<0.5	0.08	<0.3	2.0	42.5
CF12	UMU	Py	435	2600	0.005	<0.02	1.5	<2	<0.1	1.1	0.04	<0.3	0.7	37.5
CF11	UMU	Gb	65	165	0.004	0.04	1.0	<2	<0.1	1.2	0.02	<0.3	<0.4	50.0
CF10	UMU	Pe	5	2170	0.011	0.02	3.1	<2	1.10	2.5	1.15	1.4	<0.4	2.7
CF09	UMU	Gb	100	310	0.005	0.07	<1	<2	0.20	<0.5	0.06	<0.3	0.7	<16.7
CF08	UMU	Pe	5	2210	0.011	<0.02	3.1	<2	1.54	3.6	1.53	1.5	<0.4	2.0
CF07	UMU	Py	55	535	0.006	0.03	7.5	14.1	1.04	1.8	0.29	<0.3	2.4	25.9
CF06	UMU	Gb	95	635	0.004	0.04	2.5	<2	0.34	2.9	0.04	<0.3	0.8	62.5
CF05	UMU	Pe	30	2080	0.011	0.05	4.6	10.2	1.43	4.0	0.27	0.6	0.5	17.0
CF04	UMU	Py	65	1020	0.006	0.06	9.9	69.5	1.87	1.4	0.30	0.5	5.2	33.0
CF03	UMU	Pe	25	2170	0.010	<0.02	3.5	<2	1.55	2.6	1.60	1.6	<0.4	2.2
CF02	UMU	Pe	70	1410	0.014	0.06	3.5	<2	0.47	0.8	0.17	<0.3	0.7	20.6
CF01	UMU	Pe	20	2120	0.011	0.03	6.1	NA	NA	3.1	1.71	1.8	0.5	3.6

Gb = gabbroic rocks, Py = pyroxenite, Pe = peridotite, Cr = chromitite.
Cu + Ni values are reported in ppm; Co + S in wt%; PGE + Au in ppb
NA = not available

tion limits are 0.3, 0.01, 0.5, 0.1, 1, 2, and 0.4 ppb for Os, Ir, Ru, Rh, Pt, Pd, and Au, respectively. The accuracy of the data was controlled by routine analyses of the SARM–7 reference material and

in-house standards. Analytical precision, based on duplicate analyses, is better than 85%.

Results

The absolute abundance of the PGE, Au, Ni, Cu, Co, and S is reported in Table 1. PGE values are low for all rock types and are compatible with values expected in unmineralized mafic and ultramafic cumulate rocks. The data reveal higher concentrations of PGE in the Ultramafic Unit (UMU) and lower part of the Central Mafic Unit (CMU). The rocks from the upper units are largely depleted in PGE. The data also indicate characteristic chondrite-normalized PGE patterns for the various rock-types (Fig. 4).

The samples of peridotite (olivine + chromite cumulate) are mostly enriched in PGE + Au relative to samples of pyroxenite and gabbroic rocks (Table 1). The chondrite-normalized pattern is flat to slightly positive, sloping for most samples. The (Pt+Pd)/(Ru+Ir+Os) ratios are between 0.8 and 8.4 (average 3.2) and reflect the relatively high PPGE (Pd, Pt, Rh) content of the peridotites. Two anomalous PGE-enriched samples of peridotite (21 and 28) have higher (Pt+Pd)/(Ru+Ir+Os) values (17–18) and positively sloping PGE patterns. These samples form the base of large cyclic units, and they are enriched in PPGE relative to average peridotite.

The pyroxenites are websterite (opx + cpx cumulate) and orthopyroxenite (opx cumulate). They have positively sloping PGE patterns, with (Pt+Pd)/(Ru+Ir+Os) values between 2 and 35 (average 7.5). The IPGE (Os, Ir, Ru) contents and Pt/Ir ratio of pyroxenite samples are systematically lower than those of peridotite, especially for those samples from the same stratigraphic interval.

All plagioclase cumulate rocks (gabbro, gabbronorite, troctolite, olivine gabbro) are included under the generic denomination of "gabbroic rocks". They are characterized by the lowest contents of the PGE (<7.5 ppb). The PGE pattern is not well constrained owing to very low PGE contents, mostly below detection limits, but Pt/Ir values between 27 and 133 indicate a steep, positively sloping pattern.

The total PGE content of chromitite is relatively low (<200 ppb), in comparison to available data for chromitite from other layered intrusions. The PGE pattern between Os and Rh is flat, with a negative slope toward Pt and Pd. A positive slope from Pt to Pd also is characteristic of the NLI chromitite. All chromitite samples have a chondrite-normalized PGE pattern similar to that of ophiolitic chromitite (Barnes *et al.* 1985), but with relatively higher Rh content. The PGE pattern also is similar to that of chromitite from the Stillwater Complex (Naldrett & von Gruenewaldt 1989). The very high Pt and Pd contents and positively sloping PGE patterns typical of the mineralized chromitite in the Bushveld Complex, interpreted to be the result of chromitite associated with immiscible sulfides (Naldrett *et al.* 1990), are lacking in the NLI chromitite samples.

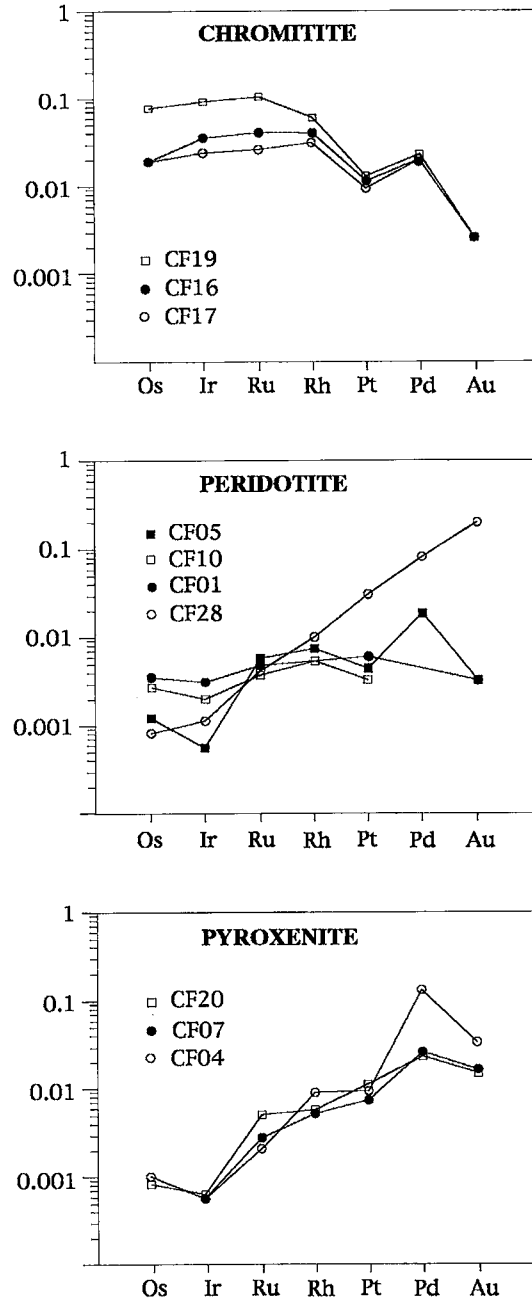

FIG. 4. Chondrite-normalized plot of PGE + Au concentrations in representative samples of the NLI. The sample numbers are those in Table 1. Normalization factors are those from C1 chondrite compiled by Naldrett & Duke (1980).

Stratigraphic distribution of PGE + Au

It can be seen from the stratigraphic distribution of total PGE contents in the NLI (Fig. 5) that higher contents of PGE are restricted to the UMU and the lower part of the CMU, with rocks from the upper units largely depleted in PGE. Decoupling of IPGE (Os, Ir, Ru) and PPGE during the early phases of crystallization can account to the concentration of Os, Ir, and Ru in the most primitive rocks, but the distribution of Pt and Pd cannot be explained in this way.

In order to evaluate the effect of rock types on the distribution of PGE in the NLI, the data were examined in terms of the rock types. The Ir–Ni plot (Fig. 6A) illustrates the higher Ni and Ir content of peridotites; pyroxenitic and gabbroic rocks are distinguished in their Ni contents, but overlap in their Ir content, although the pyroxenites generally have a higher Ir content. Considering the stratigraphic distribution of Ir across the NLI (Fig. 7), the data show that even though the chromitites and peridotites have relatively higher Ir contents (Figs. 6A, 7A, B), pyroxenites and gabbroic rocks from the UMU have higher values than those from overlying units (Fig. 7C). Both Os and Ru have similar patterns of distribution to Ir across the NLI (Figs. 8A, B). The Ir, Os, and Ru data show that

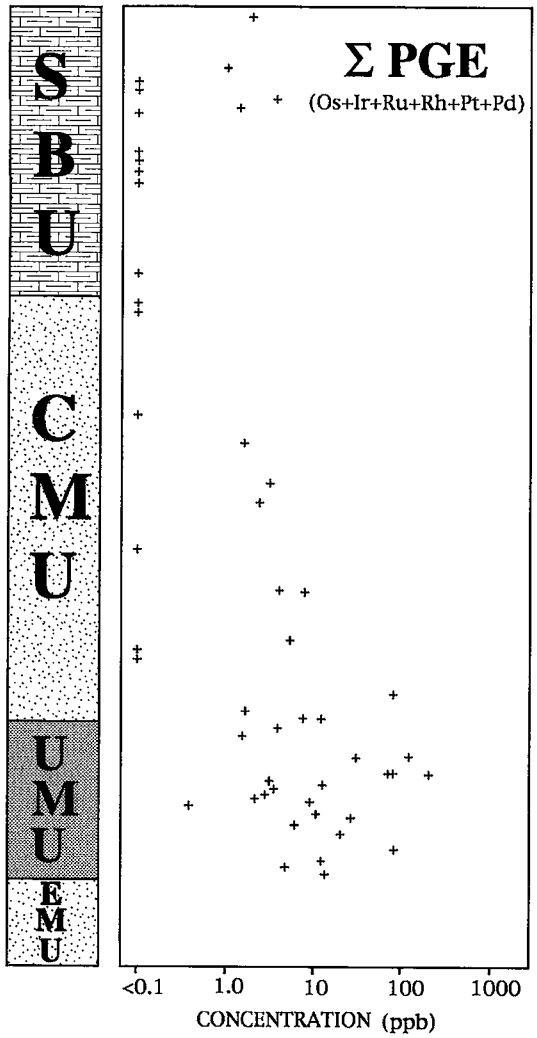

FIG. 5. Distribution of total PGE across the NLI stratigraphy. EMU: East Mafic Unit, UMU: Ultramafic Unit, CMU: Central Mafic Unit, SBU: Serra dos Borges Unit.

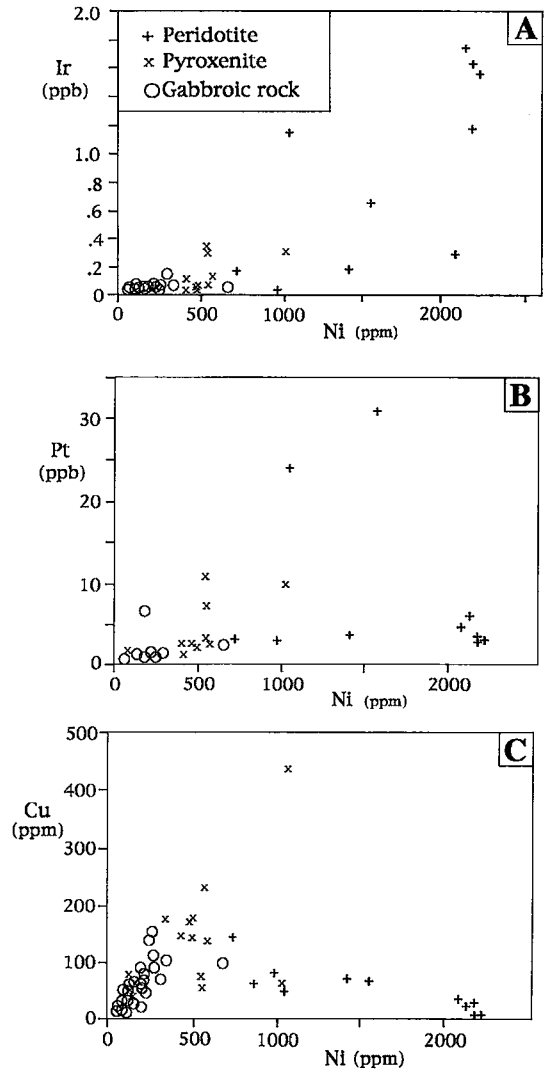

FIG. 6. Ir–Ni, Pt–Ni and Cu–Ni plots for NLI rocks.

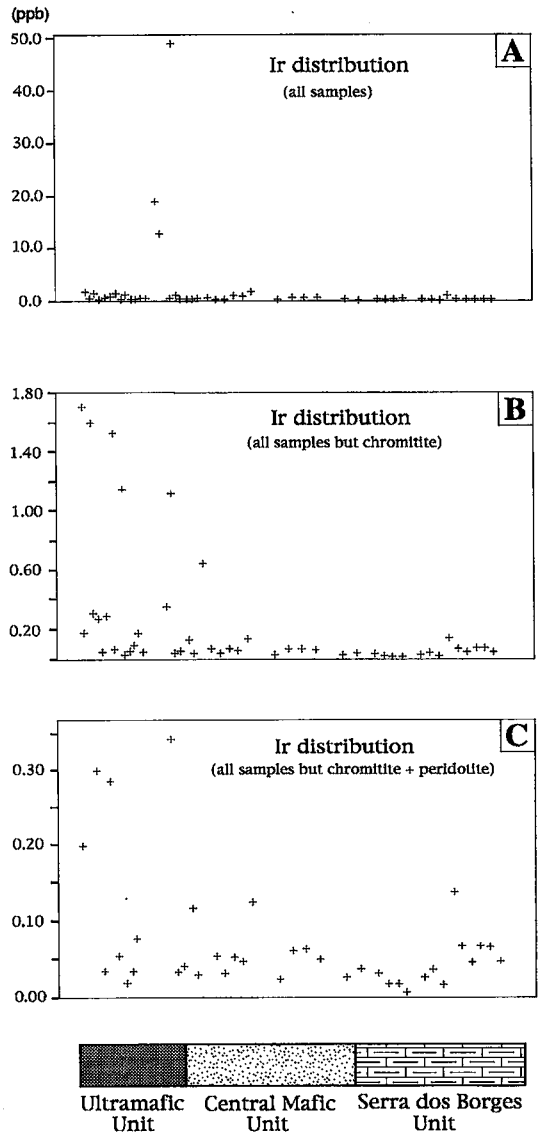

FIG. 7. Distribution of Ir across the NLI stratigraphy.

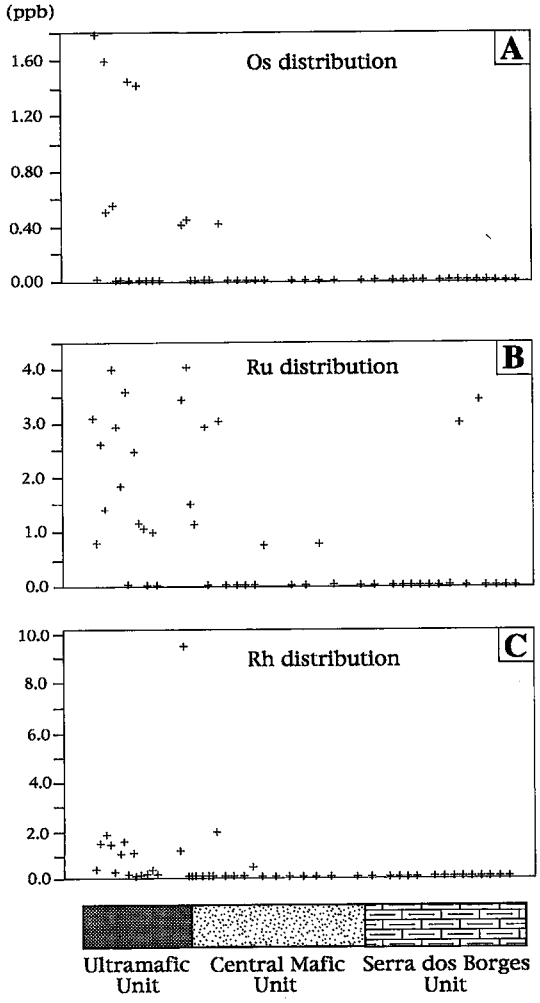

FIG. 8. Distribution of Os, Ru, and Rh across the NLI stratigraphy.

their distribution across the NLI is determined by the rock type and stratigraphic position; the highest values occur in the most primitive olivine + chromite cumulates, and, overall, the upper units are significantly depleted in these metals.

On the other hand, no correlation exists between rock type and PPGE content (Fig. 6B). Correlation coefficients for Ni–Ir in peridotite (0.71) and pyroxenite (–0.07) are distinct (Table 2), whereas correlation coefficients for Ni–Pt are similar in peridotite (–0.05) and pyroxenite (–0.09). These correlations express the affinity between Ir and the elements related to the crystallization of olivine, as well as the decoupling of Ir and Pt in the most primitive olivine-bearing cumulates. If one examines the distribution of Pt and Pd in terms of stratigraphic position within the NLI (Figs. 9A, B), the highest values are restricted to the UMU and lower part of the CMU, and the upper units are largely depleted in Pt and Pd. Au (Fig. 9C) is more scattered than the PGE; very low values occur in the upper SBU, and higher values characterize the CMU and UMU, as they do with Pt and Pd.

Rh (Fig. 8C) has a behavior that is intermediate between the IPGE and Pt–Pd. The peridotites are enriched in Rh compared to the pyroxenites and gabbroic rocks at the same stratigraphic level, but the

TABLE 2
PEARSON CORRELATION COEFFICIENTS FOR PERIDOTITE AND PYROXENITE

	Peridotites						
	Cu	Ni	Co	S	Pt	Ir	Au
Cu		-0.76 12	-0.35 12	0.86 10	0.08 11	-0.71 11	-0.06 7
Ni	0.71 13		0.59 12	-0.34 10	-0.05 11	0.71 11	-0.12 7
Co	-0.09 13	-0.27 13		-0.30 10	0.51 11	0.36 11	0.48 7
S	0.57 12	-0.02 12	0.57 12		-0.14 9	-0.44 9	-0.21 7
Pt	-0.54 11	-0.09 11	0.14 11	-0.85 10		0.12 11	0.99 7
Ir	-0.58 12	-0.07 12	-0.03 12	-0.73 11	0.97 11		0.27 7
Au	-0.58 10	-0.14 10	-0.01 10	-0.48 9	0.64 9	0.67 10	
	Pyroxenites						

Data from Table 1. Small numbers (below) refer to the number of samples.

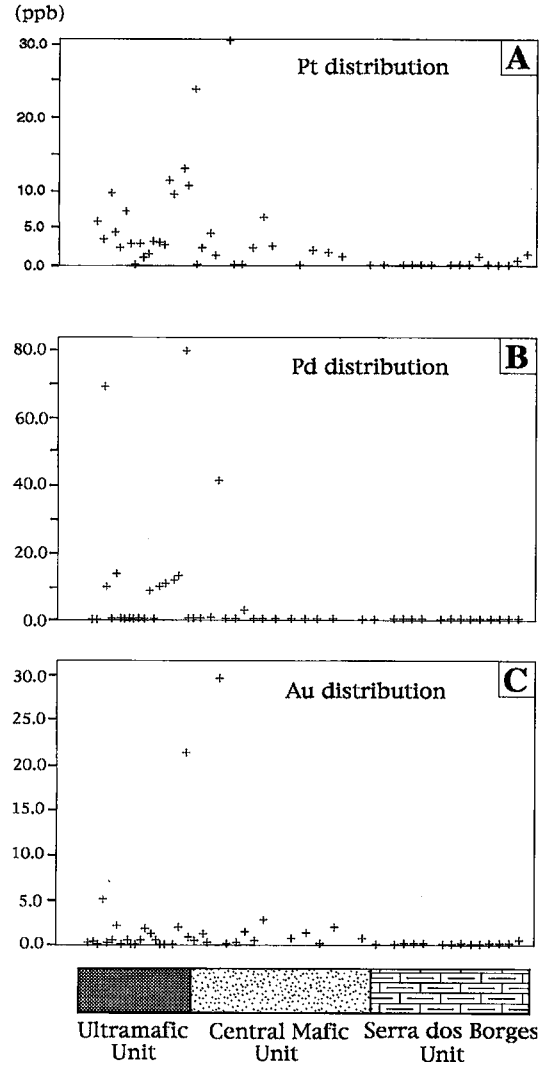

FIG. 9. Distribution of Pt, Pd, and Au across the NLI stratigraphy.

difference is less pronounced than is the case with Ir and Os. The highest values also are restricted to the UMU and lower part of the CMU, with the upper units being largely depleted in Rh.

The stratigraphic distribution of PGE across the NLI shows two important features, firstly, the compatible behavior of the IPGE in early-crystallizing high-temperature minerals, and their concentration in the more primitive olivine and chromite-bearing cumulates, and secondly, an overall pattern of higher PGE values for the UMU and the lower part of the CMU, and very low PGE contents above these units.

Ni–Cu distribution

The Ni distribution across the NLI is influenced by the abundance of olivine-rich rocks in the UMU (Figs. 10A, B). However, if the olivine cumulate rocks are removed, a strong upward depletion of Ni in the magma chamber is still indicated by the data. The zigzag distribution of Ni also suggests the replenishment of the magma chamber by new influxes of magma. This interpretation is supported by cryptic variation present in cumulus olivine in the Ultramafic Unit (Rivalenti *et al.* 1982, Girardi *et al.* 1986). The data indicate a strong fractionation of Ni during early stages in the crystallization of the magma chamber, when olivine is crystallizing.

The distribution of Cu across the NLI (Fig. 10C) shows no evidence of strong fractionation at any stage. Cu values are independent of the host rock and, with few exceptions, are uniform all across the intrusion. The exceptions are higher values in some sulfide and PGE-enriched samples. This uniform distribution of Cu indicates that either the bulk partition-coefficient for Cu remained close to 1 during crystallization or that Cu has been redistributed. It also indicates that Cu was not significantly removed from the magma by cumulus sulfide during crystallization of the NLI.

Cu and Ni have positive correlation-coefficients for gabbroic rocks and pyroxenites, but a negative correlation-coefficient for peridotites (Fig. 6C, Table 2). It is therefore suggested that Ni in peridotite is mainly hosted by olivine. This is supported by whole-rock Ni values (Table 1) compatible with Ni content of the UMU olivine (Girardi *et al.* 1986). An alternative explanation is that Cu has been preferentially removed from the sulfide component of these olivine-bearing

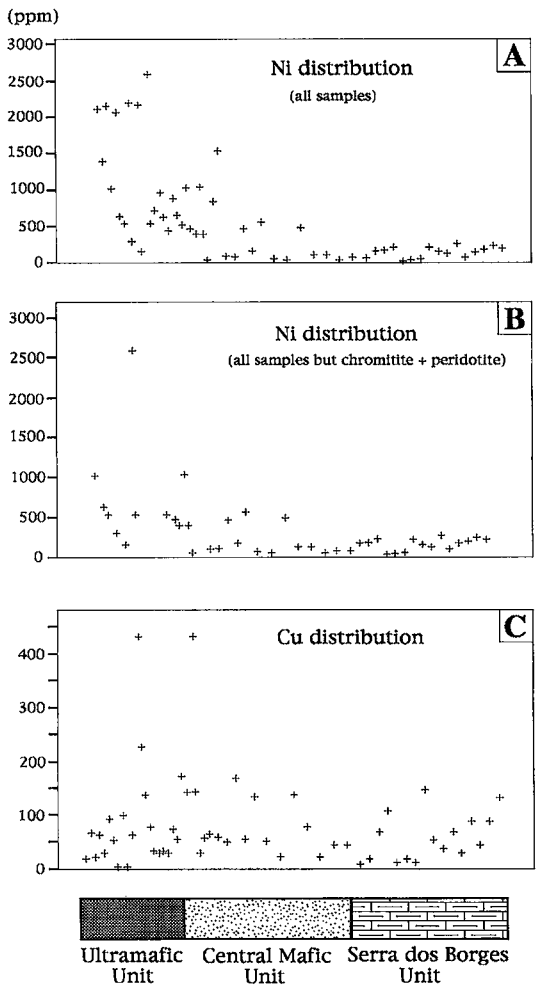

FIG. 10. Distribution of Ni and Cu across the NLI stratigraphy.

cumulates during serpentinization. Partially serpentinized peridotites have identical sulfide mineralogy compared to pyroxenitic and gabbroic rocks, which argues against serpentinization as a process responsible for the decoupling of Ni and Cu.

Sulfur

The sulfur content of the NLI cumulates is relatively high (average 490 ppm for peridotites, 1300 ppm for pyroxenites, and 760 ppm for gabbroic rocks) and reflects the ubiquitous presence of disseminated sulfides (pyrrhotite, pentlandite, chalcopyrite). Rocks with sulfides that on textural grounds seem to be cumulates (*i.e.*, those sulfides forming interstitial masses between cumulus minerals) have S content higher than 0.15–0.20 wt%. Evidence for sulfur saturation on both chemical and petrographic grounds is observed in the upper part of the UMU (Fig. 11). The low sulfide content below the upper part of the UMU is interpreted to be S trapped there as part of the intercumulus liquid. If one assumes that the content of S in the intercumulus liquid was the same as that in the parental magma, and that the porosity of the cumulates was lower than 25%, then the S content in the rocks from the lower part of the UMU (average = 0.03 wt%) indicates that the S content of the parental magma was greater than 0.12 wt%. It should be noted that the average value of 0.03 wt% S may not be exactly the original value for the cumulate rocks, because most peridotites are serpentinized, and some S may have been lost or introduced during serpentinization.

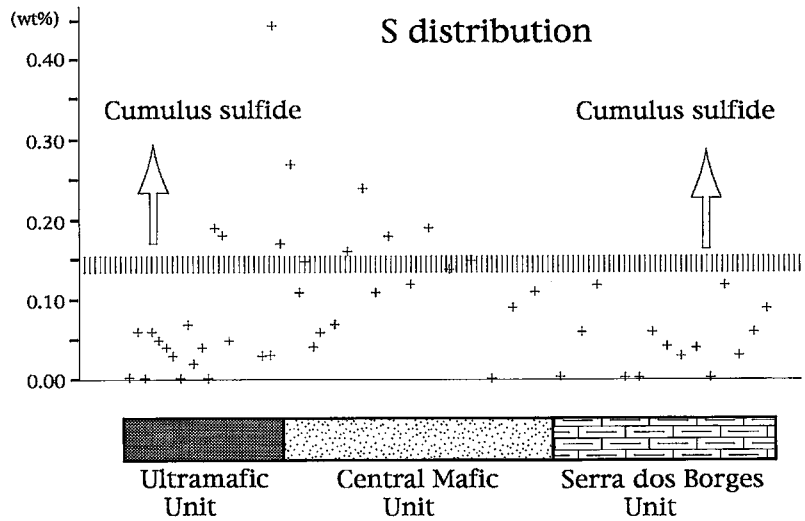

FIG. 11. Distribution of S across the NLI statigraphy. Area within and above vertical lines corresponds to samples with sulfides (po + pn + ccp) with an intercumulus texture.

Notwithstanding the inaccuracy of these estimates, they indicate relatively high contents of S in the primary magma, possibly close to levels at which magmatic sulfides are expected to form from a basaltic magma (Haughton *et al.* 1974). This suggests that the parental magma was not very far from being saturated with S, and that saturation could have been reached during the early stages of fractional crystallization. Above the upper part of the Ultramafic Unit, there is a progressive decrease in the sulfide content of the rocks, which may be interpreted as being due to the segregation of sulfides from the magma and the progressive depletion of the residual liquid. Alternatively, the progressive decrease in the sulfide content of the rocks may be caused by the increase in the FeO content and sulfur solubility of the magma.

In summary, the relatively high content of S in the lower cumulates suggests that the NLI was derived from a parental magma close to saturation with S, and that S saturation was achieved at an early stage during the fractional crystallization, as indicated by the presence of cumulus sulfides in the upper part of the UMU. Therefore, the distribution of chalcophile precious metals will be influenced by the segregation of cumulus sulfides during fractionation of the intrusion.

Postmagmatic processes

As most of our samples do not show any evidence of metamorphic recrystallization and hydrothermal alteration, the geochemical results have been so far considered as entirely related to igneous processes. It is worthy of note, however, that most samples of olivine-rich peridotite are serpentinized. The serpentinization is not associated with shear foliation, being restricted to partial replacement of olivine along fractures (Figs. 3A, C). In our samples, primary mineral and textures are always preserved, indicating a weak stage of serpentinization (Shiga 1987). Partial serpentinization, and under conditions of nonconstant volume, is mostly considered an isochemical process at hand-specimen scale (a few centimeters), except for the introduction of H_2O and loss of Ca (Coleman & Keith 1971, Eckstrand 1975, Shiga 1987). Several studies indicate that PGE are immobile during partial serpentinization (Keays & Davison 1976, Groves & Keays 1979, Oshin & Crocket 1982, Prichard & Tarkian 1988); therefore, the primary magmatic content of our samples should not be significantly affected by this alteration.

Although postmagmatic processes are not considered to be relevant to the PGE geochemistry of our samples, they certainly play an important role in the distribution of PGE in the high-grade ductile shear-zones and in the lateritic weathering profile of the NLI; these situations are not considered in this study.

Discussion

In most mineralized cumulates, the PGE are mainly associated with sulfides and have been removed from the magma in an immiscible sulfide liquid, whereas in the case of most sulfide-poor mafic and ultramafic cumulates, the picture is more complicated. The PGE grade may be due to a combination of factors, including the relative proportion of trapped intercumulus liquid and the presence or absence of cumulus sulfide and chromite. The PGE content of a cumulate rock at ppb levels probably reflects the sum of PGE concentrated in two or more different ways.

The PGE content of the magma from which a cumulate rock forms will influence its PGE content regardless of which factor is predominant with regard to the PGE content. For example, when the PGE occur in cumulate rock only as a result of trapped intercumulus liquid, the concentration of PGE present reflects the content of PGE in the magma. Similarly, the presence or absence of PGE minerals (PGM) is partly a function of the PGE content of the magma. Therefore, the average PGE content of a relatively large number of samples from different stratigraphic levels within a layered intrusion, large enough to even out variations in the proportion of trapped intercumulus liquid, and an inhomogeneous distribution of minerals and cumulus sulfides, will reflect the PGE content of the magma from which the cumulates from this horizon crystallized.

The fractionation of IPGE (Os, Ir, Ru) from PPGE (Rh, Pt, Pd) during the crystallization of mafic and ultramafic magmas in layered intrusions is now well documented (Barnes *et al.* 1985, Peck & Keays 1990). The actual mechanism responsible for this decoupling of IPGE from PPGE is uncertain, but several studies have shown the importance of chromite and olivine-bearing cumulates as concentrators of IPGE (several references in Barnes *et al.* 1988). Some authors (Keays & Campbell 1981, Barnes *et al.* 1985, Davies & Tredoux 1985) suggest that during crystallization of the most primitive cumulates, the magma becomes saturated in IPGE-bearing PGM, and the PGM are included in chromite and olivine. Support for this suggestion is provided by the common presence of IPGE-bearing inclusions in chromitite (Stockman & Hlava 1984, Talkington & Lipin 1986, Merkle 1992, Prichard *et al.* 1994), and by the presence of coarse IPGE alloys derived from boninite-related ultramafic cumulates in Tasmania (Peck *et al.* 1992). In the NLI, this effect is well illustrated in the relatively high contents of the IPGE and high IPGE/PPGE ratios in the most primitive cumulates (olivine + chromite cumulates), and low IPGE/PPGE ratios in the more evolved cumulates (pyroxenites and gabbroic rocks).

PGM have not been detected in most of our samples; this is not surprising in view of their very low PGE contents. Merkle (1992) calculated how small the

chances are of finding a grain of PGM in a single thin section in a rock with a low content of PGE. Exceptions include the chromitites from the NLI, in which PGM have been described by Ferrario & Garuti (1988) and Millioti & Stumpfl (1993); the implications of this are discussed below.

The most important result of our study is the distinction between a lower zone of the intrusion that is undepleted in PGE and an upper PGE-depleted zone. This pattern suggests that the NLI cumulates are due to crystallization from two distinct magmas insofar as their PGE content is concerned. A possible explanation for this is that the cumulates above the lower part of the CMU have crystallized from magma that resulted from influx and mixing of a new magma with a lower PGE content than that previously in the magma chamber. However, whole-rock geochemistry and cryptic variation in mineral compositions (Girardi *et al.* 1986), as well as REE patterns and La/Yb ratios (Ferreira Filho & Naldrett, in prep.) do not support the suggestion of two distinct parental magmas at this stratigraphic level. An alternative possibility is that the magma in the chamber became depleted in PGE at the transition from the UMU to the CMU. A model by which the separation of small amount of PGE-enriched sulfide liquid can cause such a depletion is developed below. This model can explain differences in PGE content in rocks that otherwise have similar and continuous petrological trends for their major and trace elements.

Model of PGE distribution

Quantitative modeling of the PGE distribution within the NLI is hampered by the absence of an unequivocal composition for the primary liquid. Thus

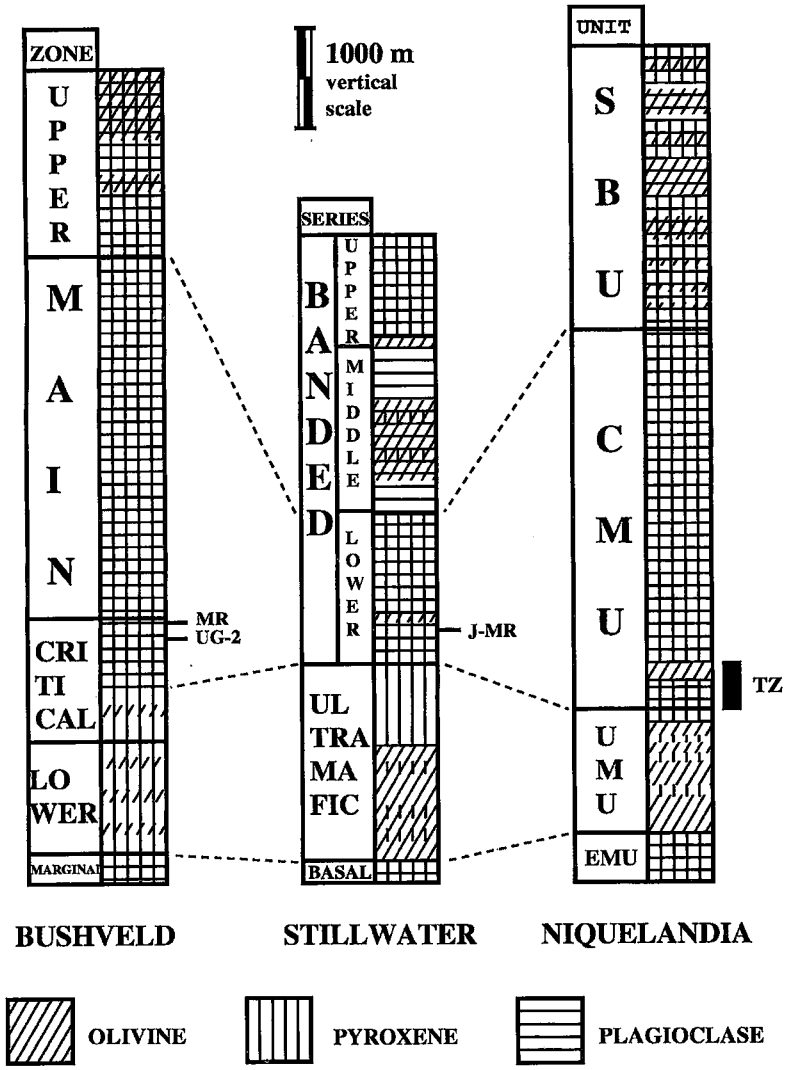

FIG. 12. Comparative generalized stratigraphy of the Bushveld, Stillwater and Niquelândia complexes. Data for Bushveld and Stillwater are from Naldrett *et al.* (1987), and data for Niquelândia from Ferreira Filho *et al.* (1992c). MR: Merensky Reef, UG–2: Upper Group chromitite 2, J–MR: J–M Reef, TZ: Transition zone from PGE-undepleted to PGE-depleted rocks.

we present a qualitative model, in which data on PGE distribution, S content, amount and texture of sulfides, and the major petrological features of the NLI, are integrated.

The model is based on Naldrett's & von Gruenewaldt's (1989) study of the variation of solubility of sulfur in increasingly fractionated magmas, such as that proposed for the Bushveld Complex. Similarities in the stratigraphy and order of appearance of the cumulus phases between the Bushveld Complex and the NLI (Fig. 12) support the use of the model, even though the composition of the parent magma in the NLI is poorly constrained. As Naldrett & von Gruenewaldt (1989) pointed out, their estimate on how the solubility of sulfur varies with fractionation of the Bushveld magma is not necessarily, and does not have to be, very accurate; however, they argued that the general shape of the solubility curve is well established and that their concept is valid as far as the general shape is correct. The model for the NLI (Fig. 13) is thus based essentially on the concave-upward shape of the sulfide-solubility curve; the general conclusions would not change even though the absolute levels of saturation of sulfide or the initial sulfur content of the parent magma may not be precise.

The initial content of iron sulfide of the primary magma has been set at 0.27 (**A** in Fig. 13). This figure is based on estimates of S content in the primary magma calculated from the amount of S introduced as trapped intercumulus liquid in the average cumulates from the lower part of the UMU, and agrees with the content of S in the tectonized gabbroic rocks of the East Mafic Unit, which is considered to represent a border group of the NLI.

If one accepts the fact that sulfide solubility varies during crystallization as predicted in Figure 13, then a sequence of major steps during fractional crystallization can be established. The lower part of the stratigraphy corresponds to rocks formed before sulfide saturation was reached (the path **A–B** in Fig. 13). As indicated by the model, olivine cumulates should predominate, with subordinate pyroxene cumulates. Successive influxes of primitive magma would have produced a pattern of dominant and thicker olivine cumulate layers with minor interlayered pyroxenite. This pattern, *i.e.*, dunite with minor interlayered pyroxenite, corresponds to what is observed in the lower part of the UMU in the NLI and is well documented petrographically (Ferreira Filho *et al.* 1992c). The hypothesis of successive influxes of primitive magma is supported by cryptic variation in the compo-

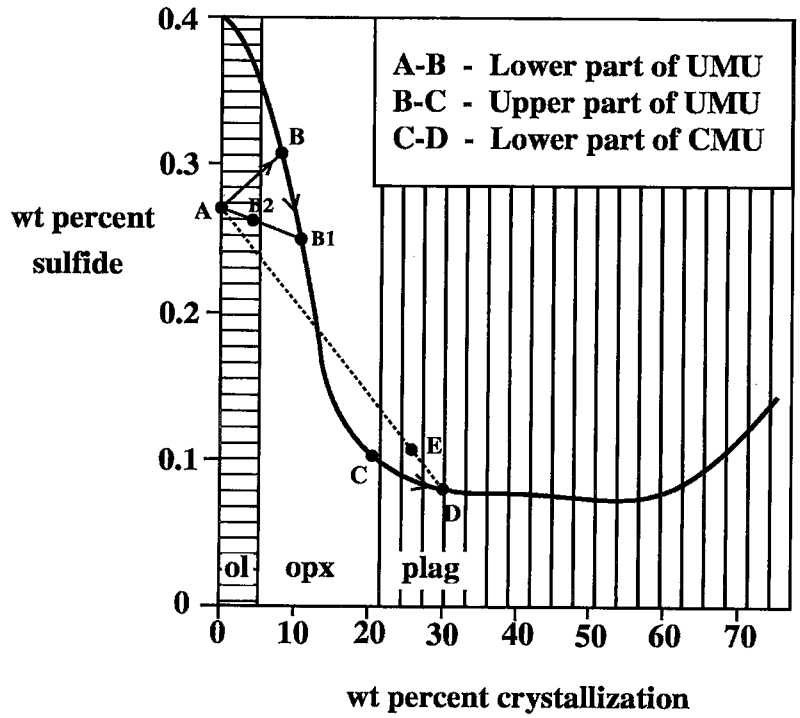

FIG. 13. Schematic diagram illustrating variation in the solubility of sulfide with fractionation. Adapted from Naldrett & von Gruenewaldt (1989). See text for discussion.

sition of olivine (Rivalenti *et al.* 1982). During this phase, the S content of the magma increased until it reached saturation (point **B**). The cumulates at this point will have an undepleted PGE content, regardless of which mechanism of collection is suggested to explain how the PGE came to be present in the rock (as part of the trapped intercumulus liquid, as PGM inclusions in cumulus phases, or both). The PGE, specially the PPGE, will become enriched as with fractional crystallization, the magma follows the path **A–B**.

After the magma has reached saturation at **B**, further crystallization will cause the segregation of sulfides and tend to deplete it in PGE. Any new influx of primitive magma will then produce an unsaturated hybrid magma along most of the path **B–C**, as is illustrated in Figure 13 by the mixing of residual liquid **B1** with primitive liquid **A** to form the hybrid magma **B2**. Successive influxes of primitive magma will result in a pattern of dominant and thicker pyroxenite layers with subordinate interlayered olivine cumulates. This is exactly what is observed in the upper part of the UMU in the NLI. The PGE depletion due to the segregation of sulfides will tend to be compensated by PGE replenishment accompanying successive influxes of new magma. The cumulates at this stage also will show undepleted PGE contents.

As crystallization proceeds beyond point **C** (Fig. 13), plagioclase will appear as a cumulus phase. The ideal situation for sulfide supersaturation due to magma mixing is present just before the magma reaches point **C**; it remains throughout the field of plagioclase crystallization. This situation is illustrated in Figure 13 by the mixing of residual magma **D** with primitive magma **A**; this gives rise to a hybrid magma **E**. A horizon close to the first appearance of cumulus plagioclase is the one most favorable for the segregation of PGE-enriched sulfide liquid, since it is here that the sulfides will segregate from magma that is least depleted in PGE. Since the sulfides form as a result of magma mixing, and since these new influxes initiate new cyclic units, the sulfides will occur at the base of these units. Successive influxes of primitive magma will result in successive cyclic units with cumulus sulfides in the more primitive rocks at the base. This situation is characteristic of the UMU to CMU transition in the NLI. At this stratigraphic level, several cyclic units were mapped, with the most primitive rocks enriched in sulfides. Furthermore, the lower part of the Central Mafic Unit marks the transition from PGE-undepleted to PGE-depleted rocks in the NLI (Fig. 5).

It can be seen from the model that plagioclase cumulates will predominate beyond point **D**. The PGE content in the plagioclase-bearing cumulates and associated pyroxenite will be very low owing to the steady depletion in PGE that periodically occurred whenever a new influx of primitive magma occurred. Cyclic units indicative of influxes of new magma are less common above the lower part of the CMU; this indicates that the magma chamber has reached a mature stage and that significant replenishment is unlikely, which accounts for the very low PGE contents in all overlying units of the NLI.

The NLI chromitites

The NLI chromitites have PGE profiles (Fig. 4) as well as (Pt+Pd)/(Os+Ir+Ru) values (Fig. 14) similar to most of the chromitites of the Stillwater Complex (Page *et al.* 1985) and some of the Lower Group chromitites in the Bushveld Complex (von Gruenewaldt *et al.* 1986, Lee & Parry 1988, Teigler 1990), but quite different to the Middle Group and Upper Group chromitites from the Bushveld Complex. The PGE content of the NLI chromitites is low compared with available data for chromitite of layered intrusions. Naldrett & von Gruenewaldt (1989) presented a model to explain the difference in the PGE content and (Pt+Pd)/(Os+Ir+Ru) value with stratigraphy in layered intrusions. The model proposes that chromitites are formed by magma mixing (as originally proposed by Irvine 1977), and that the PGE-rich chromitites are due to the former presence of an immiscible sulfide liquid. In their model, magma mixing also can account for sulfide immiscibility when a new influx of primitive magma mixes with a fractionated magma that is already crystallizing plagioclase, whereas the mixing of two relatively primitive magmas cannot. Support for this hypothesis is given by observations of PGM in chromitites; the IPGE minerals are mainly found as inclusions in chromite, whereas PPGE minerals are generally concentrated as intercumulus phases and associated with base-metal sulfides (Merkle 1992, Talkington & Lipin 1986).

Application of this model implies that the chromitites of the NLI are the result of the mixing of two relatively primitive magmas, so that sulfide saturation did not occur. The PGE in the chromitites reflect the presence Os-, Ir-, Ru-bearing PGM as inclusions in chromite, which is consistent with PGM data. The application of the model is in good agreement with the stratigraphic position of these chromitites, approximately 1 km below the appearance of cumulus plagioclase as a dominant phase, and is also supported by the similarities between the NLI chromitites and the Lower Group chromitites from the Bushveld Complex and most of the Stillwater Complex (the A chromitite from Stillwater is an exception), all of which occur below the level at which plagioclase cumulates appear in their respective intrusions.

White *et al.* (1971) reported PGE (Pt+Pd+Rh) contents of up to 3.42 ppm in the NLI chromitites from the same chromitite horizon that we sampled. The four channel samples analyzed by them, including massive

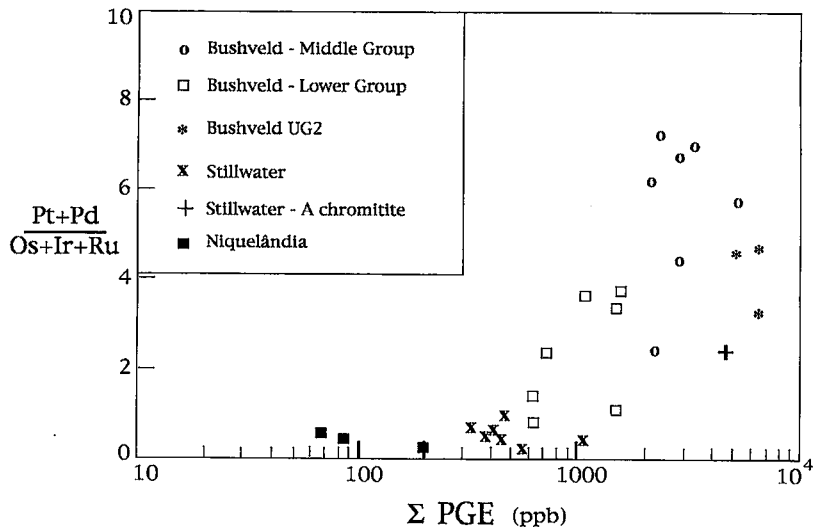

FIG. 14. Plot of total platinum-group elements *versus* (Pt+Pd)/(Os+Ir+Ru) value for chromitites. Data on Middle Group and Lower Group chromitites of the Bushveld Complex from Lee & Parry (1988), on UG2 chromitites of the Bushveld Complex from von Gruenewaldt *et al.* (1986), and on Stillwater Complex chromitites from Page *et al.* (1985); data on Niquelândia chromitites are those reported in this paper.

chromitite and weathered gangue, have variable PGE contents but systematically higher Pt and Pd values than our results. Although difficult to compare owing to the differences in the sampling and analytical methods that were used, the data of White *et al.* (1971) may be due to a possible concentration of Pt and Pd in the weathered lateritic gangue (White *et al.* 1971). Support for this suggestion is given by the observation of Pt-bearing PGM associated with goethite in holes and fractures within chromite grains (Millioti & Stumpfl 1993), which suggests remobilization of the PGE during laterization. An alternative explanation for the variance between the two sets of data is analytical variation due to the "nugget" factor of PGE-bearing sulfide or chromite grains. If the "nugget" factor is to be considered, then the larger samples collected by White *et al.* (1971) represent more accurately the PGE content of the chromitite seams than our small samples. It is worth noting that no evidence exists of PGM nuggets associated with the NLI chromitites.

IMPLICATIONS WITH RESPECT TO EXPLORATION FOR PGE DEPOSITS

The proposed model suggests that the PGE segregated from the magma chamber as the upper part of the UMU and lower part of the CMU crystallized. Such an event would be related to the segregation of cumulus sulfides, enriched in PGE, that would strip the precious metals from the magma chamber. As the rocks do not show evidence of Cu depletion associated with the observed depletion in PGE, the amount of sulfides involved in this event is likely to have been small, *i.e.*, no major massive sulfide body would have segregated, and the PGE content in the sulfides should be very high due to the high ratio of magma to sulfide accompanying this formation (Naldrett *et al.* 1987).

The scenario to be inferred from the model is very much that observed in most of the PGE-mineralized layered intrusions. It can be seen from the stratigraphic comparison between the NLI and the Bushveld and Stillwater complexes (Fig. 12) that remarkable similarities exist among these three intrusions, which further points to the possibility of similar mineralization in the NLI.

Naldrett *et al.* (1990) highlighted the fact that many PGE-enriched units occur closely associated with plagioclase-bearing rocks, within a few hundred meters of the first appearance of cumulus plagioclase as a dominant phase. Examples include the Merensky Reef and Middle and Upper Group chromitites of the Bushveld Complex, and the J–M Reef of the Stillwater Complex, all of them described by Naldrett *et al.* (1987). In the Main Sulfide Zone of the Great Dyke of

Zimbabwe (Prendergast & Keays 1989, Naldrett & Wilson 1990), the porphyritic websterite zone of the Munni Munni Complex in Western Australia (Hoatson & Keays 1989, Barnes *et al.* 1992) and the PGE-enriched sulfide zones of the Fox River Sill (Naldrett *et al.* 1995), the enriched horizons are associated with ultramafic cumulates, within a few meters (Great Dyke and Munni Munni Complex) or a few hundred meters (Fox River Sill) below the first appearance of cumulus plagioclase as a dominant phase. In all examples, the mineralization is close to the transition zone from a mainly Ultramafic Unit to a mainly Mafic Unit. It is worth stressing that at the NLI, the transition from undepleted to depleted rocks occurs close to the upward transition from ultramafic cumulates to dominantly plagioclase-bearing rocks.

The model does not necessarily indicate the presence of a PGE-bearing orebody at the transition zone from the UMU to the CMU. It merely indicates that depletion of the PGE at this stratigraphic level in the magma chamber may have been caused by the segregation of a PGE-enriched sulfide liquid. The same effect for the residual liquid in the magma chamber is expected both where a single segregation event occurs, which concentrates significant amounts of PGE in one mineralized layer, as observed in the PGE reefs, or where successive events of sulfide segregation take place, generating several layers with anomalous PGE contents but without an actual reef. Notwithstanding which of those situations took place in the NLI, the model requires that anomalous sulfide-related PGE-enriched layers be present in the upper part of the Ultramafic Unit and lower part of the Central Mafic Unit.

Acknowledgements

This project represents a portion of the senior author's Ph.D. dissertation, and was supported by grants from PADCT-CAPES (no. 2181/87) to C. F. Ferreira-Filho and NSERC operating grant A4244 to A.J. Naldrett. We thank Dr. Zoze Rosado of Cia Níquel Tocantins (Grupo Votorantim) for the facilities that enabled us to carry out the field work. Although most of the ideas presented in this paper had already been developed by the time of the "I Brazilian Meeting on Platinum Group Elements", the numerous discussions carried out during that meeting and the field trip to the Niquelândia area deeply influenced and encouraged the present work. The Organizing Committee of the PGE Brazilian Meeting is acknowledged for their invitation to the senior author to be a leader of the field trip to Niquelândia, and thus to benefit from the scientific impact of the meeting. Sylvia Araujo reviewed an earlier version of this paper. Critical review of the manuscript by Drs. Stephen J. Barnes, Robert F. Martin, and an anonymous referee is gratefully acknowledged.

References

Barnes, S.-J., Boyd, R., Korneliussen, A., Nilsson, L.-P., Often, M., Pedersen, R.B. & Robins, B. (1988): The use of mantle normalization and metal ratios in discriminating between the effects of partial melting, crystal fractionation and sulphide segregation on platinum-group elements, gold, nickel and copper: examples from Norway. *In* Geo-Platinum '87 Symp. Vol. (H.M. Prichard, P.J. Potts, J.F.W. Bowles & S.J. Cribb, eds.). Elsevier, London, U.K. (113-143).

_____, Naldrett, A.J. & Gorton, M.P. (1985): The origin of the fractionation of platinum-group elements in terrestrial magmas. *Chem. Geol.* **53**, 303-323.

Barnes, S.J., Keays, R.R. & Hoatson, D.M. (1992): Distribution of sulphides and PGE within the porphyritic websterite zone of the Munni Munni Complex, Western Australia. *Aust. J. Earth Sci.* **39**, 289-302.

Brito Neves, B.B. & Cordani, U.G. (1991): Tectonic evolution of South America during the Late Proterozoic. *Precambrian Res.* **53**, 23-40.

Coleman, R.G. & Keith, T.E. (1971): A chemical study of serpentinization – Burro Mountain, California. *J. Petrol.* **12**, 311-328.

Danni, J.C.M., Fuck, R.A. & Leonardos, O.H., Jr. (1982): Archean and Lower Proterozoic units in central Brazil. *Geol. Rundschau* **71**, 291-317.

Davies, G. & Tredoux, M. (1985): The platinum-group element and gold contents of the marginal rocks and sills of the Bushveld Complex. *Econ. Geol.* **80**, 838-848.

Eckstrand, O.R. (1975): The Dumont serpentinite: a model for control of nickeliferous opaque mineral assemblages by alteration reactions in ultramafic rocks. *Econ. Geol.* **70**, 183-201.

Ferrario, A. & Garuti, G. (1988): Platinum-group minerals in chromite-rich horizons of the Niquelândia Complex (Central Goiás, Brazil). *In* Geo-Platinum '87 Symp. Vol. (H.M. Prichard, P.J. Potts, J.F.W. Bowles & S.J. Cribb, eds.). Elsevier, London (261-272).

Ferreira Filho, C.F., Fawcett, J.J. & Naldrett, A.J. (1992a): The hercynite and quartz equilibria assemblages from the Niquelândia layered mafic–ultramafic complex, Brazil: petrology and tectonic implications. *Geol. Soc. Am., Abstr. Program* **24**, A265.

_____, Kamo, S., Fuck, R.A., Krogh, T.E. & Naldrett, A.J. (1994): Zircon and rutile geochronology of the Niquelândia layered mafic and ultramafic intrusion, Brazil: constraints for the timing of magmatism and high grade metamorphism. *Precambrian Res.* **68**, 241-255.

_____, _____, Krogh, T.E. & Naldrett, A.J. (1993): U–Pb geochronology of the Niquelândia layered mafic–ultramafic intrusion, Brazil: constraints for the timing of magmatism and high grade metamorphism. *Geol. Assoc. Can. – Mineral. Assoc. Can., Program Abstr.* **18**, A30.

——— & NALDRETT, A.J. (1993): The Niquelândia mafic–ultramafic complex revisited: tectonic setting and potential for PGE deposits. *In* First Brazilian PGE Meeting, Extended Abstr. Vol., 25-28.

———, ——— & FAWCETT, J.J. (1992b): Prograde metamorphism in the Niquelândia layered complex, Brazil: evidence for an oblique cross-section through the continental crust. *Geol. Soc. Am., Abstr. Program* **24**, A179.

———, NILSON, A.A. & NALDRETT, A.J. (1992c): The Niquelândia mafic–ultramafic complex, Goiás, Brazil: a contribution to the ophiolite × stratiform controversy based on new geological and structural data. *Precambrian Res.* **59**, 125-143.

FIGUEIREDO, A.N. (1977): Depósitos de cromita de Goiás e Campo Formoso (BA): diagnose e análise comparativa. *Rev. Bras. Geoc.* **7**, 73-83.

FUCK, R.A., PIMENTEL, M.M. & BOTELHO, N.F. (1987): Granitoid rocks in west-central Brazil: a review. Int. Symp. on Granites and Associated Mineralizations (Salvador), SGRM/SBG, 53-59.

GIRARDI, V.A.V., RIVALENTI, G. & SINIGOI, S. (1986): The petrogenesis of the Niquelândia layered basic–ultrabasic complex, central Goiás, Brazil. *J. Petrol.* **27**, 715-744.

GROVES, D.I. & KEAYS, R.R. (1979): Mobilization of ore-forming elements during alteration of dunites, Mt. Keith – Betheno, Western Australia. *Can. Mineral.* **17**, 373-389.

HAUGHTON, D.R., ROEDER, P.L. & SKINNER, B.J. (1974): Solubility of sulfur in mafic magmas. *Econ. Geol.* **69**, 451-467.

HOATSON, D.M. & KEAYS, R.R. (1989): Formation of platiniferous sulfide hirizons by crystal fractionation and magma mixing in the Munni Munni Layered Intrustion, West Pilbara Block, Western Australia. *Econ. Geol.* **84**, 1775-1804.

IRVINE, T.N. (1977): Origin of chromitite layers in the Muskox intrusion and other stratiform intrusions: a new interpretation. *Geology* **5**, 273-277.

KEAYS, R.R. & CAMPBELL, I.H. (1981): Precious metals in the Jimberlana Intrusion, Western Australia: implications for the genesis of platiniferous ores in layered intrusions. *Econ. Geol.* **76**, 1118-1141.

——— & DAVISON, R.M. (1976): Palladium, iridium and gold in the ores and host rocks of nickel sulfide deposits in Western Australia. *Econ. Geol.* **71**, 1214-1228.

LEE, C.A. & PARRY, S.J. (1988): Platinum-group element geochemistry of the Lower and Middle Group chromitites of the Eastern Bushveld Complex. *Econ. Geol.* **83**, 1127-1139.

MARINI, O.J., FUCK, R.A., DANNI, J.C.M., DARDENNE, M.A., LOGUERCIO, S.O.C. & RAMALHO, R. (1984): As faixas de dobramentos Brasília, Uruaçu e Paraguai–Araguaia e o Maciço Mediano de Goiás. *In* Geologia do Brasil (C. Schobbenhaus, coord.). MME-DNPM, 251-303.

MERKLE, R.K.W. (1992): Platinum-group minerals in the middle group of chromitite layers at Marikana, western Bushveld Complex: indications for collection mechanisms and postmagmatic modification. *Can. J. Earth Sci.* **29**, 209-221.

MILLIOTI, C.A. & STUMPFL, E.F. (1993): Platinum-group mineral inclusions, textures and distribution in the chromitites of the Niquelândia Complex, Brazil. *First Brazilian PGE Meeting, Extended Abstr. Vol.*, 33-35.

NALDRETT, A.J., ASIF, M., SCOATES, R.J.F., ECKSTRAND, O.R. & SCHWANN, P.L. (1994): Platinum-group elements in Fox River Sill, Manitoba, Canada: implications with respect to influxes of fresh magma and exploration for PGE deposits. *Trans. Inst. Mining Metall.* **103**, B10-B21.

———, BRÜGMANN, G.E. & WILSON, A.H. (1990): Models for the concentration of PGE in layered intrusions. *Can. Mineral.* **28**, 389-408.

———, CAMERON, G., VON GRUENEWALDT, G. & SHARPE, M.R. (1987): The formation of stratiform PGE deposits in layered intrusions. *In* Origins of Igneous Layering (I. Parsons, ed.). NATO Adv. Study Inst. Ser. **C 196**, 313-397.

——— & DUKE, J.M. (1980): Platinum metals in magmatic sulphide ores. *Science* **208**, 1417-1424.

——— & VON GRUENEWALDT, G. (1989): Association of platinum-group elements with chromitite in layered intrusions and ophiolite complexes. *Econ. Geol.* **84**, 180-187.

——— & WILSON, A.H. (1990): Horizontal and vertical variations in noble-metal distribution in the Great Dyke of Zimbabwe: a model for the origin of the PGE mineralization by fractional segregation of sulfide. *Chem. Geol.* **88**, 279-300.

OSHIN, I.O. & CROCKET, J.H. (1982): Noble metals in Thetford Mines ophiolites, Quebec, Canada. I. Distribution of gold, iridium, platinum, and palladium in the ultramafic and gabbroic rocks. *Econ. Geol.* **77**, 1556-1570.

PAGE, N.J., ZIENTEK, M.L., CZAMANSKE, K. & FOOSE, M.P. (1985): Sulfide mineralization in the Stillwater Complex and underlying rocks. *Montana Bur. Mines Geol., Spec. Publ.* **92**, 93-96.

PECK, D.C. & KEAYS, R.R. (1990): Insights into the behavior of precious metals in primitive, S-undersaturated magmas: evidence from the Heazlewood River Complex, Tasmania. *Can. Mineral.* **28**, 553-577.

_____, _____ & FORD, R.J. (1992): Direct crystallization of refractory platinum-group element alloys from boninitic magmas: evidence from western Tasmania. *Aust. J. Earth Sci.* **39**, 373-387.

PIMENTEL, M.M., HEAMAN, L. & FUCK, R.A. (1992): Idade do meta-riolito da Sequência Maratá, Grupo Araxá, Goiás: estudo geocronológico pelos métodos U–Pb em zircão, Rb–Sr e Sm–Nd. *An. Acad. Bras. Ciências* **64**, 19-28.

_____, _____, _____ & MARINI, O.J. (1991): U–Pb geochronology of Precambrian tin-bearing continental-type acid magmatism in central Brazil. *Precambrian Res.* **52**, 321-335.

PRENDERGAST, M.D. & KEAYS, R.R. (1989): Controls of platinum-group mineralization and the origin of the PGE-rich Main Sulfide Zone in the Wedza Subchamber of the Great Dyke, Zimbabwe: implications for the genesis of, and exploration for, stratiform PGE mineralization in layered intrusion. *In* Magmatic Sulfides – The Zimbabwe Volume (M.D. Prendergast & M.J. Jones, eds.). *Inst. Mining Metall., Spec. Publ.*, 21-42.

PRICHARD, H.M., IXER, R.A., LORD, R.A., MAYNARD, J. & WILLIAMS, N. (1994): Assemblages of platinum-group minerals and sulfides in silicate lithologies and chromite-rich rocks within the Shetland ophiolite. *Can. Mineral.* **32**, 271-294.

_____ & TARKIAN, M. (1988): Platinum and palladium minerals from two PGE-rich localities in the Shetland Ophiolite Complex. *Can. Mineral.* **26**, 979-990.

RIVALENTI, G., GIRARDI, V.A.V., SINIGOI, S., ROSSI, A. & SIENA, F. (1982): The Niquelândia mafic–ultramafic complex of central Goiás, Brazil: petrological considerations. *Rev. Bras. Geoc.* **12**, 380-391.

SIGHINOLFI, G.P., GIRARDI, V.A.V., RIVALENTI, G., SINIGOI, S. & ROSSI, A. (1983): PGE, Au and Ag distribution in the Precambrian Niquelândia Complex, central Goiás, Brazil. *Rev. Bras. Geoc.* **13**, 52-55.

SHIGA, Y. (1987): Behavior of iron, nickel, cobalt and sulfur during serpentinization, with reference to the Hayachine ultramafic rocks of the Kamaishi mining district, northeastern Japan. *Can. Mineral.* **25**, 611-624.

STOCKMAN, H.W. & HLAVA, P.F. (1984): Platinum-group minerals in Alpine chromitites from southwestern Oregon. *Econ. Geol.* **79**, 491-508.

TALKINGTON, R.W. & LIPIN, B. (1986): Platinum-group minerals in chromite seams of the Stillwater Complex, Montana. *Econ. Geol.* **81**, 1179-1186.

TEIGLER, B. (1990): Platinum group element distribution in the Lower and Middle Group chromitites in the Western Bushveld Complex. *Mineral. Petrol.* **42**, 165-179.

VON GRUENEWALDT, G., HATTON, C.J., MERKLE, R.K.W. & GAIN, S.B. (1986): Platinum-group element-chromitite associations in the Bushveld Complex. *Econ. Geol.* **81**, 1067-1079.

WHITE, R.W., MOTTA, J. & DE ARAUJO, V.A., (1971): Platiniferous chromitite in the Tocantins complex, Niquelândia, Goiás, Brazil. *U.S. Geol. Surv., Prof. Pap.* **750**, D26-D33.

Received December 21, 1993, revised manuscript accepted August 5, 1994.

APPENDIX 1. Modal composition

			volume %							
Sample	Unit	Rock	ol	opx	cpx	pl	chr	Fe-Ti ox	Sulfides	Alteration
CF54	SBU	ol-gabbro	20		16	64			diss., Po+Ccp+Pn	corona
CF53	SBU	ol-gabbro	19		20	61			diss., Po+Ccp+Pn	corona
CF52	SBU	ol-gabbro	19	2	21	58			rare, diss., Po+Ccp+Pn	corona
CF51	SBU	ol-gabbronorite	5	16	33.5	45		0.5	diss., Po+Ccp+Pn	corona
CF50	SBU	gabbronorite		25	25	49.5		0.5		
CF49	SBU	ol-gabbro	15	4	19	62			rare, diss., Po+Ccp+Pn	corona
CF48	SBU	websterite		40	56	4			rare, diss., Po+Ccp+Pn	
CF47	SBU	websterite		41	56	3			rare, diss., Po+Ccp+Pn	
CF46	SBU	ol-gabbro	19	7	32	42			rare, diss., Po+Ccp+Pn	corona
CF45	SBU	anorthosite			3	97				
CF44	SBU	anorthosite			2	98				
CF43	SBU	ol-gabbro	20		25	55			diss., Po+Ccp+Pn	corona
CF42	SBU	ol-gabbro	15		25	60			rare, diss., Po+Ccp+Pn	corona
CF41	SBU	gabbronorite		18	29.5	52		0.5		
CF40	CMU	gabbronorite		24	28	47		1	diss., Po+Ccp+Pn	
CF39	CMU	gabbronorite		20	21	48		1	diss., Po+Ccp+Pn	
CF38	CMU	gabbronorite		30	27	40		3		
CF37	CMU	websterite		59	38	3			int., Po+Ccp+Pn	
CF36	CMU	websterite		56	40	4			int., Po+Ccp+Pn	
CF35	CMU	gabbronorite		28.5	15	56		0.5	diss., Po+Ccp+Pn	
CF34	CMU	gabbronorite		25	19.5	55		0.5	diss., Po+Ccp+Pn	
CF33	CMU	plg-websterite		68	27	5			int., Po+Ccp+Pn	
CF32	CMU	gabbronorite		28	24	48			diss., Po+Ccp+Pn	
CF31	CMU	websterite		71	28	1			int., Po+Ccp+Pn	
CF30	CMU	gabbronorite		28	23.5	46		0.5	diss., Po+Ccp+Pn	
CF29	CMU	gabbronorite		32	18	49.5		0.5	diss., Po+Ccp+Pn	
CF28	CMU	dunite	98				2		diss., Po+Ccp+Pn	Serp.
CF27	CMU	harzburgite	52	42	4.5		1.5		diss., Po+Ccp+Pn	Serp.
CF26	CMU	gabbronorite		19	29	51.5		0.5	diss., Po+Ccp+Pn	
CF25	CMU	websterite		61	39				diss., Po+Ccp+Pn	
CF24	CMU	websterite		77	23				int., Po+Ccp+Pn	
CF23	UMU	websterite		58	39	3			int., Po+Ccp+Pn	
CF22	UMU	websterite		57	43				int., Po+Ccp+Pn	
CF21	UMU	harzburgite	83	15			2		rare, diss., Po+Ccp+Pn	Serp.
CF20	UMU	ol-websterite	7	71	11		1		rare, diss., Po+Ccp+Pn	
CF19	UMU	chromitite					100			Weath.
CF18	UMU	chromitite					100			Weath.
CF17	UMU	chromitite					100			Weath.
CF16	UMU	chromitite					100			Weath.
CF15	UMU	lherzolite	48	43	7		2		diss., Po+Ccp+Pn	Serp.
CF14	UMU	lherzolite	45.5	27	26		1.5		int., Po+Ccp+Pn	Serp.
CF13	UMU	websterite		55	45				int., Po+Ccp+Pn	
CF12	UMU	websterite		58	42					
CF11	UMU	gabbronorite		22	18	60			diss., Po+Ccp+Pn	
CF10	UMU	dunite	90	8			2			Serp.
CF09	UMU	gabbronorite		28	20	52			diss., Po+Ccp+Pn	
CF08	UMU	harzburgite	85	12	1.5		1.5			Serp.
CF07	UMU	websterite	8	61	30		1		rare, diss., Po+Ccp+Pn	
CF06	UMU	gabbronorite		29	25	46			rare, diss., Po+Ccp+Pn	
CF05	UMU	dunite	90	6			4		diss., Po+Ccp+Pn	Serp.
CF04	UMU	ol-websterite	8	68	23.5		0.5		diss., Po+Ccp+Pn	
CF03	UMU	harzburgite	88	10.5			1.5		rare, diss., Po+Ccp+Pn	Serp.
CF02	UMU	dunite	90	8			2		diss., Po+Ccp+Pn	Serp.
CF01	UMU	dunite	89	9			2		rare, diss., Po+Ccp+Pn	Serp.

ol = olivine, opx = orthopyroxene, cpx = clinopyroxene, pl = plagioclase, chr = Cr-spinel, Fe-Ti ox. = Fe-Ti spinel
Po = pyrrhotite, Ccp = chalcopyrite, Pn = pentlandite, diss = disseminated, int = interstitial
serp. = partial serpentinization of olivine, weath. = sample partially weathered, corona = reaction corona between ol and pl.